

Measuring the neutrino mass from future wide galaxy cluster catalogues

Carmelita Carbone

Dipartimento di Astronomia, Alma Mater Studiorum-Università di Bologna, via Ranzani 1, I-40127 Bologna, Italy
§ INAF-Osservatorio Astronomico di Bologna, Via Ranzani 1, I-40127, Bologna, Italy
§ INFN, Sezione di Bologna, Viale Berti Pichat 6/2, I-40127 Bologna, Italy
carmelita.carbone@unibo.it

Cosimo Fedeli

Department of Astronomy, University of Florida, 211 Bryant Space Science Center, Gainesville, FL 32611
cosimo.fedeli@astro.ufl.edu

Lauro Moscardini

Dipartimento di Astronomia, Alma Mater Studiorum-Università di Bologna, via Ranzani 1, I-40127 Bologna, Italy
§ INAF-Osservatorio Astronomico di Bologna, Via Ranzani 1, I-40127, Bologna, Italy
§ INFN, Sezione di Bologna, Viale Berti Pichat 6/2, I-40127 Bologna, Italy
lauro.moscardini@unibo.it

Andrea Cimatti

Dipartimento di Astronomia, Alma Mater Studiorum-Università di Bologna, via Ranzani 1, I-40127 Bologna, Italy
§ INAF-Osservatorio Astronomico di Bologna, Via Ranzani 1, I-40127, Bologna, Italy
a.cimatti@unibo.it

ABSTRACT: We present forecast errors on a wide range of cosmological parameters obtained from a photometric cluster catalogue of a future wide-field *Euclid*-like survey. We focus in particular on the total neutrino mass as constrained by a combination of the galaxy cluster number counts and correlation function. For the latter we consider only the shape information and the Baryon Acoustic Oscillations (BAO), while marginalising over the spectral amplitude and the redshift space distortions. In addition to the cosmological parameters of the standard Λ CDM+ ν model we also consider a non-vanishing curvature, and two parameters describing a redshift evolution for the dark energy equation of state. For completeness, we also marginalise over a set of “nuisance” parameters, representing the uncertainties on the cluster mass determination. We find that combining cluster counts with power spectrum information greatly improves the constraining power of each probe taken individually, with errors on cosmological parameters being reduced by up to an order of magnitude. In particular, the best improvements are for the parameters defining the dynamical evolution of dark energy, where cluster counts break degeneracies. Moreover, the resulting error on neutrino mass is at the level of $\sigma(M_\nu) \sim 0.9$ eV, comparable with that derived from present Ly α forest measurements and Cosmic Microwave background (CMB) data in the framework of a non-flat Universe. Further adopting *Planck* priors and reducing the number of free parameters to a Λ CDM+ ν cosmology allows to place constraints on the total neutrino mass of $\sigma(M_\nu) \sim 0.08$ eV, close to the lower bound enforced by neutrino oscillation experiments. Finally, in the optimistic case where uncertainties in the calibration of the mass-observable relation were so small to be neglected, the combination of *Planck* priors with cluster counts and power spectrum would constrain the total neutrino mass down to $\sigma(M_\nu) \sim 0.034$ eV, i.e. the minimum neutrino mass predicted by oscillation experiments would be detected in a Λ CDM framework. We thus show that galaxy clusters from future wide galaxy surveys will be an excellent tool for studying cosmology and fundamental physics.

Contents

1. Introduction	1
2. Clusters: effective bias and mass function	3
2.1 Nuisance parameters	4
3. Cosmological model with massive neutrinos	6
4. Forecast approach: combining cluster BAO and counts	7
4.1 Fisher matrix for BAO+ $\mathbf{P}_c(\mathbf{k})$ -shape	7
4.2 Fisher matrix for cluster counts	9
4.3 <i>Euclid</i> -like survey	9
5. Results	10
5.1 BAO+CMB	11
5.2 COUNTS+CMB	14
5.3 BAO+COUNTS	15
5.4 BAO+COUNTS+CMB	15
6. Conclusions	16
A. The observed galaxy cluster power spectrum	18
B. The <i>Planck</i> Fisher matrix	20

1. Introduction

It is now established from solar, atmospheric, reactor and accelerator experiments that neutrinos have non-zero mass, and that a lower limit on the total neutrino mass is given by $M_\nu \equiv \sum m_\nu \sim 0.05$ eV [1, 2], where m_ν is the mass of a single neutrino species. On the other hand the individual masses are still unknown. Since neutrino mass affects the evolution of the Universe in several observable ways, its measurements can be obtained from different cosmological probes, such as observations of the CMB, galaxy clustering, Ly α forest, and weak lensing data [3, 4, 5, 6].

In particular, a thermal neutrino relic component in the Universe impacts both the expansion history and the growth of cosmic structures. Neutrinos with mass $\lesssim 0.6$ eV become non-relativistic after the epoch of recombination probed by the CMB, and this mechanism allows massive neutrinos to alter the matter-radiation equality for a fixed $\Omega_m h^2$. Massive neutrinos act as non-relativistic particles on scales $k > k_{\text{nr}} = 0.018(m_\nu/1\text{eV})^{1/2}\Omega_m^{1/2}h/\text{Mpc}$,

where k_{nr} is the wave-number corresponding to the Hubble horizon size at the epoch z_{nr} when the given neutrino species becomes non-relativistic, Ω_m is the matter energy density and $h = H_0/100 \text{ km s}^{-1} \text{ Mpc}^{-1}$. The large velocity dispersion of non-relativistic neutrinos suppresses the formation of neutrino perturbations in a way that depends on m_ν and redshift z , leaving an imprint on the matter power spectrum for scales $k > k_{\text{fs}}(z) = 0.82H(z)/H_0/(1+z)^2(m_\nu/1\text{eV})h/\text{Mpc}$ [1, 7], where neutrinos cannot cluster and do not contribute to the gravitational potential wells produced by cold dark matter and baryons. This modifies the shape of the matter power spectrum and the correlation function on these scales [8, 9, 10, 11, 12, 13, 14].

Massive neutrinos affect also the CMB statistics. WMAP7 alone constrains $M_\nu < 1.3$ eV [15] and data from the ACT¹ and SPT² experiments constrain $M_\nu < 0.948$ eV in the framework of a non-flat cosmology [16]. Furthermore, thanks to the improved sensitivity to polarisation and to the angular power spectrum damping tail, forecasts for the *Planck* satellite alone give a $1\text{-}\sigma$ error on the total neutrino mass of $\sim 0.2 - 0.4$ eV, depending on the assumed cosmological model and fiducial neutrino mass [17, 18]. Moreover, the combination of present data-sets from CMB and large-scale structure (LSS) yields an upper limit of $M_\nu < 0.3$ eV [19, 20, 21, 22, 23]. A further robust constraint on neutrino masses has been obtained using the Sloan Digital Sky Survey flux power spectrum alone, finding an upper limit of $M_\nu < 0.9$ eV (2σ C. L.) [24]. However, the tightest constraints to date in terms of a 2σ upper limit on the neutrino masses have been obtained by combining the Sloan Digital Sky Survey flux power from the Ly α forest with CMB and galaxy clustering data. These constraints are partly driven by a discrepancy in the measured σ_8 between Ly α forest and CMB, and result in $\Sigma m_\nu < 0.17$ eV [25]. Somewhat less constraining bounds have been obtained by [26], while for forecasts on future CMB and Ly α forest joint constraints we refer to [27].

Moreover, the forecast sensitivity of future LSS experiments, when combined with *Planck* CMB priors, indicates that observations should soon be able to detect signatures of the cosmic neutrino background and measure the neutrino mass even in the case of the minimum mass $M_\nu = 0.05$ eV [18, 28, 29, 30, 31, 32]. Furthermore, these future surveys have been planned to measure with high accuracy the so-called “dark energy” equation of state. In fact, there is now strong evidence that the current energy density of the Universe is dominated by dark energy with an equation of state $w \sim -1$, which is causing accelerated expansion. Accordingly, in this work we consider, in addition to massive neutrinos, the effect on LSS of a homogeneous dark energy component with a general time-varying equation of state $w(z)$.

In this respect, Ref. [32] has shown that future spectroscopic galaxy surveys, such as the ESA selected mission *Euclid*³ [33], will be capable of estimating the neutrino mass scale independently of flatness assumptions and dark energy parametrisation, if the total neutrino mass M_ν is > 0.1 eV. On the other hand, if M_ν is < 0.1 eV, the sum of neutrino masses, and in particular the minimum neutrino mass required by neutrino oscillations,

¹<http://www.phy.princeton.edu/act/>

²<http://pole.uchicago.edu/>

³<http://www.euclid-ec.org/>

can be measured in the context of a Λ CDM model. For further discussion on neutrino mass constraints from different probes see e.g. [2, 3] and references therein.

In this picture, little attention has been dedicated to the constraining potential of galaxy clusters. Historically these systems have played a fundamental role in cosmology. For instance, the correlation function of galaxy clusters provided the very first hint toward the low-density Universe that is today commonly accepted as the standard cosmological model [34, 35]. Galaxy cluster number counts at high-redshift later provided yet another early evidence for the matter density parameter being substantially smaller than unity [36, 37]. Galaxy clusters trace the large-scale matter distribution much as galaxies, with the difference that the former have a substantially larger bias than the latter, and hence their correlation is a factor of a few higher. At the same time, clusters are relatively rare objects, therefore their abundance is highly sensitive to features in the primordial matter power spectrum. These occurrences make clusters in principle valuable tools for constraining the details of the cosmological model, and in particular the neutrino masses. However their low spatial number density is also a drawback, in that it increases substantially the shot noise and the Poisson noise as compared to galaxies. Their effective cosmological power hence depends significantly on the chosen selection function and on the precision with which cluster masses can be estimated. In this work we study how the combination of cluster number counts with the shape of the cluster power spectrum, including information from the BAO, can constrain the total neutrino mass. We focus on the cluster catalogue that will be produced by the photometric part of *Euclid*, and provide constraints on the parameter set of an extended cosmological model which includes curvature, massive neutrinos, and a time-varying dark energy component. Since deviations from the standard model in the form of extra neutrino species are still uncertain [38, 39], in this paper we focus on standard neutrino families only and analyse the constraining power that future galaxy cluster catalogues, photometrically selected from galaxy surveys of *Euclid*-type, have on the total neutrino mass.

The rest of the paper is organised as follows. In § 2 we present the galaxy cluster modelling adopted in this work and the modifications due to uncertainties in the calibration of the mass-observable relation. In § 3 we describe the adopted fiducial model and the effect of massive neutrinos on the matter power spectrum. In § 4 we review our forecasting approach as applied to cluster counts and power spectrum, and specify characteristics of the galaxy cluster survey analysed in this work. In § 5 we present our results on the forecast neutrino mass errors, and finally in § 6 we draw our conclusions.

2. Clusters: effective bias and mass function

In the cosmological analysis performed in this paper we combine number counts and the power spectrum of galaxy clusters. These are identified as overdensities of galaxies photometrically selected with a *Euclid*-type survey. In order to properly define the relevant cluster catalogue we adopt the minimum mass $M_{\min}(z)$ provided by the *Euclid Red-Book* [33] for objects identified as having a S/N ratio larger than 5. Let us assume a perfect knowledge of the mass of each cluster in the catalogue for the time being. This assump-

tion will be relaxed in § 2.1 below. The resulting (full-sky equivalent) cluster redshift distribution can then be computed as

$$\frac{dN(z)}{dz} = \frac{dV(z)}{dz} g(z) , \quad (2.1)$$

where $dV(z)/dz$ is the cosmic volume per unit redshift, while

$$g(z) \equiv \int_{M_{\min}(z)}^{+\infty} dM n(M, z) . \quad (2.2)$$

For the mass function $n(M, z)$ of dark matter halos we adopt the prescription given by [40], which is based on an approximated ellipsoidal collapse model and has been shown to agree well with the results of numerical cosmological simulations. Although derived in a Λ CDM context, this prescription has been shown to model $n(M, z)$ accurately even in the presence of dynamic dark energy [41, 42] and massive neutrinos [43, 14, 44], and holds, in particular, for the fiducial values of neutrino mass and dark energy parameters considered in this work (see §3).

As for the power spectrum of galaxy clusters, we simply assume it to be a biased version of the linear dark matter power spectrum. Nonlinear effects become important on scales $k \gtrsim 0.1 h \text{ Mpc}^{-1}$, which at low redshift have been disregarded in our Fisher matrix analysis, as we shall explain in Appendix A. By assuming again a perfect knowledge of the cluster masses in the *Euclid* catalogue, we can compute the power spectrum as $P(k, z) = b_e^2(z) P_L(k, z)$, where $P_L(k, z)$ is the linear dark matter power spectrum, while $b_e(z)$ is the effective bias of clusters in the catalogue, defined as

$$b_e(z) \equiv \frac{1}{g(z)} \int_{M_{\min}(z)}^{+\infty} dM n(M, z) b(M, z) . \quad (2.3)$$

In Eq. (2.3), the function $b(M, z)$ represents the bias of dark matter halos, for which we adopt the semi-analytic prescription of [45] (see [43] for an analysis of this prescription against N-body simulations which include a massive neutrino component). We compute the linear dark matter power spectrum $P_L(k, z)$ with the publicly available software package CAMB [46], which takes correctly into account the effect of massive neutrinos.

2.1 Nuisance parameters

The discussion presented in § 2 assumes a perfect knowledge of the true mass of clusters in our catalogue. This is a very strong assumption, in that reliable mass estimates can be obtained only with an extensive multi-wavelength follow-up and only for the most massive objects. A less expensive alternative, particularly suitable for large cluster catalogues, is to adopt a scaling relation between the observable quantity at hand (cluster richness in this case) and the true underlying mass. Scaling relations between cluster properties are however not perfect one-to-one associations; they include a scatter and, in some circumstances, systematic biases. In order to take properly into account the uncertainties that a scaling relation introduces in the knowledge of the true underlying mass, we treat the

scatter and systematic biases as “nuisance” parameters, and marginalise over them in the Fisher matrix analysis for cluster counts in § 4.2.

Given this, let $p(M_o|M)$ be the probability that for a given cluster of intrinsic mass M we infer the mass M_o through the scaling relation [47]. The redshift distribution of clusters given by Eq. (2.2) above then gets modified according to

$$g(z) = \int_{M_{\min}(z)}^{+\infty} dM_o \int_0^{+\infty} dM n(M, z) p(M_o|M). \quad (2.4)$$

By assuming a lognormal scatter around the nominal scaling relation with dispersion $\sigma_{\ln M}$, the probability can be written as

$$p(M_o|M) = \frac{1}{M_o \sqrt{2\pi} \sigma_{\ln M}} \exp[-x^2(M_o)], \quad (2.5)$$

where

$$x(M_o) \equiv \frac{1}{\sqrt{2}\sigma_{\ln M}} [\ln(M_o) - B_M - \ln(M)]. \quad (2.6)$$

Evidently, the parameter B_M represents the fractional value of a systematic bias in the scaling relation. It easily follows that the function $g(z)$ can then be simplified to

$$g(z) = \frac{1}{2} \int_0^{+\infty} dM n(M, z) \operatorname{erfc}[x(M_{\min}(z))], \quad (2.7)$$

where $\operatorname{erfc}(x)$ is the complementary error function [48].

Likewise, the effective bias presented in Eq. (2.3) now takes the more general form

$$b_e(z) = \frac{1}{2g(z)} \int_0^{+\infty} dM n(M, z) b(M, z) \operatorname{erfc}[x(M_{\min}(z))]. \quad (2.8)$$

It is straightforward to verify that, in the ideal case in which the systematic bias $B_M \rightarrow 0$ and the scatter $\sigma_{\ln M} \rightarrow 0$, the expressions for the cluster redshift distribution and the effective bias reduce to their simplest form, presented at the beginning of §2. In what follows we adopt these updated forms for the cluster redshift distribution and the effective bias.

Moreover, following [47], we assume the following redshift parametrisation for the halo mass bias and variance:

$$\begin{aligned} \ln B_M(z) &= A + B \ln(1+z) \\ \sigma_{\ln M}^2(z) &= \sigma_{\ln M,0}^2 - 1 + (1+z)^{2\beta}. \end{aligned} \quad (2.9)$$

In this way, we have four nuisance parameters, namely A , B , $\sigma_{\ln M,0}$ and β . For the reference model, we assume $\ln B_M(z)$ to be zero at $z = 0$ (i.e. $A = 0$), with no evolution (i.e. $B = 0$), but leaving A and B as free parameters with Gaussian priors of $\sigma(A) = \sigma(B) = 0.25$ [49], which is not overly restrictive for *Euclid* [33]. In Eq. (2.9), we have also allowed for a power-law redshift evolution for the variance $\sigma_{\ln M}^2(z)$ of the lognormal intrinsic scatter around the nominal scaling relation. Ref. [50] estimates that $\sigma_{\ln M,0} = 0.2$ and we choose $\beta = 0.125$. This means that the scatter will grow to a value of 0.6 at a redshift of $z = 2$. In

the count Fisher matrix analysis we self-calibrate for these scatter variables with Gaussian priors of $\sigma(\sigma_{\ln M,0}) = 0.1$ [51] and $\sigma(\beta) = 0.1$, which should be conservative estimates, although these quantities are unconstrained by present data [33]. It is expected that Stage III surveys, e.g. DES⁴, will shed light on this quantity beyond redshift $z = 1$.

As mentioned above, for the minimum cluster mass as a function of redshift $M_{\min}(z)$, we adopt the prescription detailed in the *Euclid Red-Book* [33] for the photometric cluster catalogue. The redshift evolution of the cluster number counts is computed in bins of width $\Delta z = 0.1$ between $z = 0.2$ and $z = 2$, and we integrate the cluster distribution over mass, considering number counts in redshift-space only. Concerning redshift errors that enter the observed galaxy cluster power spectrum, better described in Appendix A, we assume that photometrically selected clusters will be spectroscopically confirmed up to $z = 1$.

3. Cosmological model with massive neutrinos

According to the latest observations (e.g. [15, 52] and refs. therein), we assume the following fiducial cosmological model at the present epoch: $\Omega_m = 0.271$, $\Omega_\Lambda = 1 - \Omega_m$, $h = 0.703$, $A_s = 2.525 \times 10^{-9}$, $\Omega_b = 0.045$, $n_s = 0.966$, $w_0 = -0.95$, $w_a = 0$, $M_\nu \equiv \sum_i m_{\nu_i} = 0.05 \text{eV}$ ⁵. This corresponds to $\sigma_8 = 0.8$ for the fiducial cosmology. We consider neither primordial gravitational waves nor a scale dependent component of the scalar spectral index, and assume the matter energy density Ω_m to include the baryon and neutrino contributions when neutrinos are non-relativistic, so that $\Omega_m = \Omega_c + \Omega_b + \Omega_\nu$, where $\Omega_\nu = M_\nu / (93.14 h^2 \text{eV})$ [53].

In our fiducial cosmology, the dark energy is described by a cosmic fluid with an equation of state $w_{de}(z) = p_{de}(z) / \rho_{de}(z)$, where p_{de} and ρ_{de} are the pressure and energy density of the dark energy fluid, respectively. The redshift dependent dark energy density is then

$$\rho_{de}(z) = \rho_{de}(0) \exp \left[3 \int_0^z \frac{1 + w(z')}{1 + z'} dz' \right] \quad (3.1)$$

which we normalise so that $\Omega_{de} = \Omega_\Lambda$ at the present epoch. Finally, to compute our forecasts on dark energy parameters, we adopt the widely used linear dark energy equation of state $w_{de}(a) = w_0 + (1 - a)w_a$ [54, 55], where $a \equiv 1/(1 + z)$ is the scale factor normalised to unity at present. When the dark energy equation of state is a function of redshift, as we assume in the present work, the constraints on the the sum of neutrino masses can degrade significantly, since dark energy and massive neutrinos both affect the growth rate of structures [56]. However, as we will show in § 5, the combination of CMB and galaxy cluster data reduces or even breaks these degeneracies.

As we have mentioned in § 1, massive neutrinos suppress the matter power spectrum on wave-numbers above the free-streaming scale k_{fs} , while on very large scales they behave as ordinary cold dark matter. The suppression effect is encapsulated in the parameter $f_\nu \equiv$

⁴<http://www.darkenergysurvey.org/>

⁵Here we assume an effective number of neutrino species $N_{\text{eff}} = 3.04$ and, since neutrino oscillation experiments have shown that at least one neutrino species is heavier than 0.05 eV, we consider an inverted hierarchy where $m_1 \sim m_2, m_3 \sim 0$

Ω_ν/Ω_m , which damps the source of matter density perturbations. In fact, the linear growth rate is defined as $f_g \equiv d \ln \delta / d \ln a$, where δ represents the matter density perturbation $\delta \equiv \delta \rho_m / \rho_m$, and ρ_m and $\delta \rho_m$ the matter density and the overdensity, respectively. In the presence of massive neutrinos and a dark energy component the equation for the linear evolution of matter density perturbations on scales $k \gg k_{\text{fs}}$ can be written as [57, 41]

$$\frac{df_g}{d \ln a} = -f_g^2 - \left\{ 1 - \frac{1}{2} [\Omega_m(a) + (3w_{de}(a) + 1)\Omega_{de}(a)] \right\} f_g + \frac{3}{2} \Omega_m(a)(1 - f_\nu), \quad (3.2)$$

where $\Omega_m(a) = H_0^2 \Omega_m a^{-3} / H^2(a)$ and $\Omega_{de}(a) = H_0^2 \Omega_\Lambda X(a) / H^2(a)$ are the time-dependent density parameters of matter and dark energy, respectively. Here $H(a) = H_0(\Omega_{rad}^{-4} + \Omega_m a^{-3} + \Omega_K a^{-2} + \Omega_\Lambda X(a))^{1/2}$, where, for the parametrisation of the dark energy equation of state chosen above, we have $X(a) = a^{-3(1+w_0+w_a)} \exp(3w_a(a-1))$ [58].

Eq. (3.2) is a simplified description of the effect of massive neutrinos on the growth of structures, since in the presence of massive neutrinos the growth rate is not only redshift-dependent, but also *scale*-dependent. For this reason, in the present work we have computed f_g using the semi-analytic formula of Ref. [57], as we explain in Appendix A.

4. Forecast approach: combining cluster BAO and counts

In this work we derive neutrino constraints combining measurements from a *Euclid*-like galaxy cluster catalogue with CMB measurements as obtained from a *Planck*-like CMB experiment⁶. To this aim, we adopt a Fisher matrix approach [59] that allows us to forecast cosmological parameter errors from LSS and CMB. In order to compute CMB priors we use the specifications of the *Planck* satellite and, as explained in Appendix B, we describe CMB temperature and polarisation power spectra using the parameter set $\boldsymbol{\theta} = \{\omega_m, \omega_b, \omega_\nu, 100\theta_S, \log(10^{10} A_s), n_S, \tau\}$, where θ_S is the angular size of the sound horizon at last scattering, and τ is the optical depth due to reionisation. After marginalising over the optical depth, we propagate the *Planck* CMB Fisher matrix F_{ij}^{CMB} into the final sets of parameters \mathbf{q} adopted in § 4.1, using the appropriate Jacobian for the involved parameter transformation.

4.1 Fisher matrix for BAO+ $P_c(\mathbf{k})$ -shape

In this section we apply, to the observed galaxy cluster power spectrum, the so-called “ $P(k)$ method marginalised over growth information”, which exploits only the shape and the BAO positions of the cluster power spectrum, while marginalising over amplitude and redshift-space distortions. This method allows us to estimate, from the galaxy cluster catalogue, measurements of the cosmological parameters which characterise the underlying fiducial cosmology. Up to now, this method has been applied to the galaxy power spectrum in a number of works (see e.g., [32, 60, 61, 62, 63, 64, 65, 66, 67]). Here we present the main formulae describing this approach, referring to Appendix A for details.

⁶www.rssd.esa.int/index.php?project=planck

Including redshift-space distortions and the geometrical effects due to the incorrect assumption of the reference cosmology with respect to the true one [60], the observed galaxy cluster power spectrum can be written as

$$P_{\text{obs}}(k_{\text{ref}\perp}, k_{\text{ref}\parallel}, z) = \frac{D_A(z)_{\text{ref}}^2 H(z)}{D_A(z)^2 H(z)_{\text{ref}}} P_c(k_{\text{ref}\perp}, k_{\text{ref}\parallel}, z) + P_{\text{shot}}, \quad (4.1)$$

where P_c is given by Eq. (A.4) and $D_A(z)$, $H(z)$, k_{\perp} , k_{\parallel} are defined in Appendix A.

We divide the survey volume into redshift shells with size $\Delta z = 0.1$, centred at redshift z_i , and choose the following set of parameters to describe $P_{\text{obs}}(k_{\text{ref}\perp}, k_{\text{ref}\parallel}, z)$:

$$\{H(z_i), D_A(z_i), \bar{G}(z_i), \beta(z_i, k), P_{\text{shot}}^i, \omega_m, \omega_b, \omega_\nu, n_s, h\}, \quad (4.2)$$

where $\omega_\nu \equiv \Omega_\nu h^2$, $\omega_m = \Omega_m h^2$, $\omega_b = \Omega_b h^2$. Finally, since the growth factor $G(z)$, the effective bias $b_e(z)$, and the power spectrum normalisation P_0 are completely degenerate, we introduce the quantity $\bar{G}(z_i) = (P_0)^{0.5} b_e(z_i) G(z_i) / G(z_0)$ [62].

Under the assumptions discussed in Appendix A, the Fisher matrix associated to the observed galaxy cluster power spectrum can be approximated as [68, 69]

$$\begin{aligned} F_{ij}^{\text{P}_c} &= \int_{\vec{k}_{\text{min}}}^{\vec{k}_{\text{max}}} \frac{\partial \ln P_{\text{obs}}(\vec{k})}{\partial p_i} \frac{\partial \ln P_{\text{obs}}(\vec{k})}{\partial p_j} V_{\text{eff}}(\vec{k}) \frac{d\vec{k}}{2(2\pi)^3} \\ &= \int_{-1}^1 \int_{k_{\text{min}}}^{k_{\text{max}}} \frac{\partial \ln P_{\text{obs}}(k, \mu)}{\partial p_i} \frac{\partial \ln P_{\text{obs}}(k, \mu)}{\partial p_j} V_{\text{eff}}(k, \mu) \frac{2\pi k^2 dk d\mu}{2(2\pi)^3}, \end{aligned} \quad (4.3)$$

where the derivatives are evaluated at the parameter values p_i of the fiducial model, and V_{eff} is the effective volume of the survey:

$$V_{\text{eff}}(k, \mu) = \left[\frac{n_c P_c(k, \mu)}{n_c P_c(k, \mu) + 1} \right]^2 V_{\text{survey}}. \quad (4.4)$$

Here we have assumed that the comoving galaxy cluster number density n_c is constant in position and given by Eq. (2.7). Due to azimuthal symmetry around the line of sight, the three-dimensional galaxy cluster power spectrum $P_{\text{obs}}(\vec{k})$ depends only on k and μ , i.e. it is reduced to two dimensions by symmetry [60].

We do not include information from the amplitude $\bar{G}(z_i)$ and the redshift space distortions $\beta(z_i, k)$, so we marginalise over these parameters and also over P_{shot}^i . Then we project $\mathbf{p} = \{H(z_i), D_A(z_i), \omega_m, \omega_b, \omega_\nu, n_s, h\}$ into the final sets \mathbf{q} of cosmological parameters [70],

$$\mathbf{q} = \{\Omega_m, \Omega_K, \Omega_b, h, M_\nu, n_s, w_0, w_a, \log(10^{10} A_s)\}. \quad (4.5)$$

The transformation from one set of parameters to another is given by

$$F_{\alpha\beta}^{\text{P}_c} = \sum_{ij} \frac{\partial p_i}{\partial q_\alpha} F_{ij}^{\text{P}_c} \frac{\partial p_j}{\partial q_\beta}, \quad (4.6)$$

where $F_{\alpha\beta}^{\text{P}_c}$ is the survey Fisher matrix for the set of parameters \mathbf{q} , and $F_{ij}^{\text{P}_c}$ is the survey Fisher matrix for the set of equivalent parameters \mathbf{p} .

The adopted full $P(k)$ method marginalised over growth information does not give any constraint on A_s , since the normalisation of the cluster power spectrum is marginalised over. Therefore, the $\log(10^{10} A_s)$ -errors shown in § 5 come from combining cluster counts and CMB measurements.

4.2 Fisher matrix for cluster counts

Following the approach of [71, 72, 73, 74, 75], the Fisher matrix for the number of clusters, N_i , within the i -th redshift bin and mass $M > M_{\min}(z)$, can be written as

$$F_{\alpha\beta}^N = \sum_i \frac{\partial N_i}{\partial \tilde{q}_\alpha} \frac{\partial N_i}{\partial \tilde{q}_\beta} \frac{1}{N_i}, \quad (4.7)$$

where the sum over i runs over redshift intervals and the number of clusters expected in a survey having a sky coverage $\Delta\Omega$ in the redshift range between z_i and z_{i+1} can be written as

$$N_i = \Delta\Omega \int_{z_i}^{z_{i+1}} dz \frac{dV}{dz d\Omega} g(z). \quad (4.8)$$

Here $g(z)$ is given by Eq. (2.7), dV/dz is the cosmology-dependent comoving volume element per unity redshift interval and solid angle, and finally, the cosmological parameter set \tilde{q}_α is given by

$$\tilde{\mathbf{q}} = \{\Omega_m, \Omega_K, \Omega_b, h, M_\nu, n_s, w_0, w_a, \log(10^{10} A_s), A, B, \sigma_{\ln M, 0}, \beta\}. \quad (4.9)$$

Where not otherwise specified, we marginalise over the four nuisance parameters A , B , $\sigma_{\ln M, 0}$, and β to obtain the constraints on q_α of Eq. (4.5) from cluster counts. It is worth noting that in Eq. (4.7) we have adopted the same approach of Ref. [75], i.e. we integrate the cluster distribution over mass and consider number counts in redshift-space only, in order to reduce the effects due to the model-dependence of the cluster mass inference.

Having defined the Fisher matrices $F_{\alpha\beta}$ for CMB, $P_c(k)$, and N_i , respectively, the $1-\sigma$ error on q_α , marginalised over the other parameters, is $\sigma(q_\alpha) = \sqrt{(F^{-1})_{\alpha\alpha}}$. Furthermore, to quantify the level of degeneracy between the different parameters, we estimate the so-called correlation coefficients, given by

$$r \equiv \frac{(F^{-1})_{\alpha\beta}}{\sqrt{(F^{-1})_{\alpha\alpha}(F^{-1})_{\beta\beta}}}. \quad (4.10)$$

When the coefficient $|r| = 1$ the two parameters are totally degenerate, while $r = 0$ means they are uncorrelated.

In § 5 we shall evaluate $\sigma(q_\alpha)$ and r both from galaxy cluster data, $F_{\alpha\beta}^{\text{Pc}}$, $F_{\alpha\beta}^{\text{N}}$, $F_{\alpha\beta}^{\text{Pc}} + F_{\alpha\beta}^{\text{N}}$, and from their combination with CMB priors, $F_{\alpha\beta}^{\text{Pc}} + F_{\alpha\beta}^{\text{CMB}}$, $F_{\alpha\beta}^{\text{N}} + F_{\alpha\beta}^{\text{CMB}}$, $F_{\alpha\beta}^{\text{Pc}} + F_{\alpha\beta}^{\text{N}} + F_{\alpha\beta}^{\text{CMB}}$.

4.3 *Euclid*-like survey

In this work we forecast neutrino constraints using count and power spectrum measurements of galaxy clusters photometrically selected by a future survey like the one planned by the ESA selected M-class *Euclid* galaxy survey. This survey will be able to push towards very high redshifts over a large area, thanks to its unique capabilities in the infrared which cannot be matched from the ground. Conservative estimates, based on simulated mock catalogues, indicate that *Euclid* will find of order $\sim 6 \times 10^4$ clusters with S/N better than 3, between $z = 0.2$ and $z = 2.0$, with 10^4 at $z > 1$ [33]. In this case, the

Table 1: Forecast $1-\sigma$ errors for the cosmological parameters considered in the text and the corresponding correlations r with M_ν , for a *Euclid*-like experiment alone and in combination with *Planck*.

General cosmology												
	BAO		BAO+CMB		COUNTS ^a		COUNTS ^a +CMB		BAO+COUNTS ^a		BAO+COUNTS ^a +CMB	
	σ	r	σ	r	σ	r	σ	r	σ	r	σ	r
Ω_m	0.4139	0.7470	0.0437	0.1278	0.1560	0.8588	0.0275	-0.3193	0.0356	-0.0869	0.0106	0.4046
Ω_K	1.3327	-0.3479	0.0302	0.1003	2.6134	-0.2491	0.0069	-0.2102	0.4189	0.0849	0.0039	0.3854
Ω_b	0.1008	0.6507	0.0072	0.0083	1.0042	-0.5785	0.0050	-0.4842	0.0143	-0.6459	0.0016	0.0125
h	0.3955	0.6583	0.0562	-0.0158	7.3604	0.5735	0.0386	0.4771	0.0411	-0.5120	0.0125	-0.0380
M_ν	2.5972	1.0000	0.2283	1.0000	28.513	1.0000	0.2564	1.0000	0.8905	1.0000	0.1853	1.0000
n_s	0.5332	-0.2732	0.0024	-0.0666	4.0365	-0.6573	0.0024	-0.0486	0.1452	0.8252	0.0024	-0.0297
w_0	1.7820	0.05685	1.4648	-0.0248	0.4659	0.0997	0.2381	-0.2154	0.3157	-0.2136	0.2133	0.0020
w_a	6.6788	-0.2651	5.4101	-0.0044	5.3758	-0.4089	0.8187	0.0374	1.0644	-0.2882	0.7218	-0.2123
$\log(10^{10} A_s)$	–	–	0.0253	0.9117	2.2631	0.9057	0.0287	0.9336	0.2899	0.1826	0.0222	0.8878

Λ CDM												
	BAO		BAO+CMB		COUNTS ^a		COUNTS ^a +CMB		BAO+COUNTS ^a		BAO+COUNTS ^a +CMB	
	σ	r	σ	r	σ	r	σ	r	σ	r	σ	r
Ω_m	0.1131	0.2559	0.0038	-0.8535	0.0461	0.7086	0.0087	-0.9673	0.0252	0.3455	0.0036	-0.8361
Ω_b	0.0308	-0.2015	0.0010	-0.7291	0.6646	0.0628	0.0021	-0.9401	0.0107	-0.4618	0.0009	-0.7042
h	0.0935	-0.2121	0.0071	0.8008	4.7404	0.3998	0.0162	0.9561	0.0310	-0.4705	0.0068	0.7796
M_ν	1.7791	1.0000	0.0818	1.0000	4.2971	1.0000	0.1679	1.0000	0.5686	1.0000	0.0758	1.0000
n_s	0.3100	0.7894	0.0023	0.2498	1.4125	-0.6499	0.0023	-0.0576	0.0713	0.5757	0.0023	0.2220
$\log(10^{10} A_s)$	–	–	0.0140	0.6771	0.9446	0.2623	0.0225	0.9122	0.1021	0.8754	0.0138	0.7522

^aThe four nuisance parameters, A , B , $\sigma_{\ln M,0}$, and β have been marginalised over.

cluster-based constraints on cosmological parameters will be limited by the understanding of the catalogue selection function, systematic errors and cluster mass determinations and their uncertainties. In this respect, *Euclid* will be able to calibrate the mass-observable relations and their scatter through lensing measurements. The high image quality and number density of sources will enable *Euclid* to measure masses of clusters much more accurately and out to higher redshifts than is possible from the ground. Moreover, the combination of *Euclid* data with other surveys, such as eROSITA⁷ or Planck, will enable the cross-calibration of non-lensing mass-observable relations, which are currently limited to low redshifts and small samples. For instance, *Euclid* will provide mass proxies via the stacking of clusters according to their X-ray or Sunyaev-Zel'dovich signals. [33]. Here we adopt the following specification for the *Euclid*-like galaxy cluster catalogue analysed in this work: $\text{area} = 15 \times 10^3 \text{ deg}^2$, $z_{\min} = 0.2$, $z_{\max} = 2$, $\Delta_z = 0.1$, $S/N > 5$.

5. Results

In this Section we present the predicted $1-\sigma$ marginalised errors and correlations for the cosmological parameter set, described in Eq. (4.5), considered in this work, focusing in

⁷<http://www.mpe.mpg.de/erosita/>

Table 2: Comparison of the *Euclid*+*Planck* forecast 1- σ errors and the corresponding correlations with M_ν , for different treatments of the nuisance parameters.

General cosmology				
	BAO+COUNTS ^a +CMB		BAO+COUNTS ^b +CMB	
	σ	r	σ	r
Ω_m	0.0106	0.4046	0.0057	0.6860
Ω_K	0.0039	0.3854	0.0031	0.6551
Ω_b	0.0016	0.0125	0.0008	0.3456
h	0.0125	-0.0380	0.0061	-0.3841
M_ν	0.1853	1.0000	0.1064	1.0000
n_s	0.0024	-0.0297	0.0023	0.0722
w_0	0.2133	0.0020	0.1477	0.7178
w_a	0.7218	-0.2123	0.5119	-0.7616
$\log(10^{10} A_s)$	0.0222	0.8878	0.0175	0.8599

Λ CDM				
	BAO+COUNTS ^a +CMB		BAO+COUNTS ^b +CMB	
	σ	r	σ	r
Ω_m	0.0036	-0.8361	0.0008	0.1401
Ω_b	0.0009	-0.7042	0.0003	0.5604
h	0.0068	0.7796	0.0021	-0.3582
M_ν	0.0758	1.0000	0.0339	1.0000
n_s	0.0023	0.2220	0.0023	0.5414
$\log(10^{10} A_s)$	0.0138	0.7522	0.0103	0.9441

^aThe four nuisance parameters, $B_{M,0}$, $\sigma_{\ln M,0}$, α , and β have been marginalised over.

^bThe four nuisance parameters, $B_{M,0}$, $\sigma_{\ln M,0}$, α , and β have been kept fixed to the fiducial values reported in the text.

particular on the total neutrino mass M_ν . As explained in § 3, we have assumed an inverted mass hierarchy with a fiducial $M_\nu = 0.05$ eV, which represents the minimum total neutrino mass predicted by neutrino oscillation experiments. In this respect, we have been very conservative, and consequently the forecast $\sigma(M_\nu)$ errors should be viewed as upper bounds for neutrino mass measurements in the context of a *Euclid*-like galaxy cluster survey in combination with *Planck*.

In Table 1 we show the marginalised errors for the cosmological parameters of Eq. (4.5) and the corresponding correlation coefficients with M_ν , for the different probes and their combinations analysed in this work. Moreover, Figs. 1-2 represent the corresponding 2-parameter M_ν - q_α joint contours at 68% C.L. Finally, in Table 2 we compare the cosmological parameter errors and their correlations with M_ν as obtained from galaxy cluster measurements in combination with CMB data, for the two different cases in which the nuisance parameters $B_{M,0}$, $\sigma_{\ln M,0}$, α and β are kept fixed to their fiducial values or are marginalised over.

5.1 BAO+CMB

Let us consider the different probes separately. The 2nd and 3rd columns of the upper panel

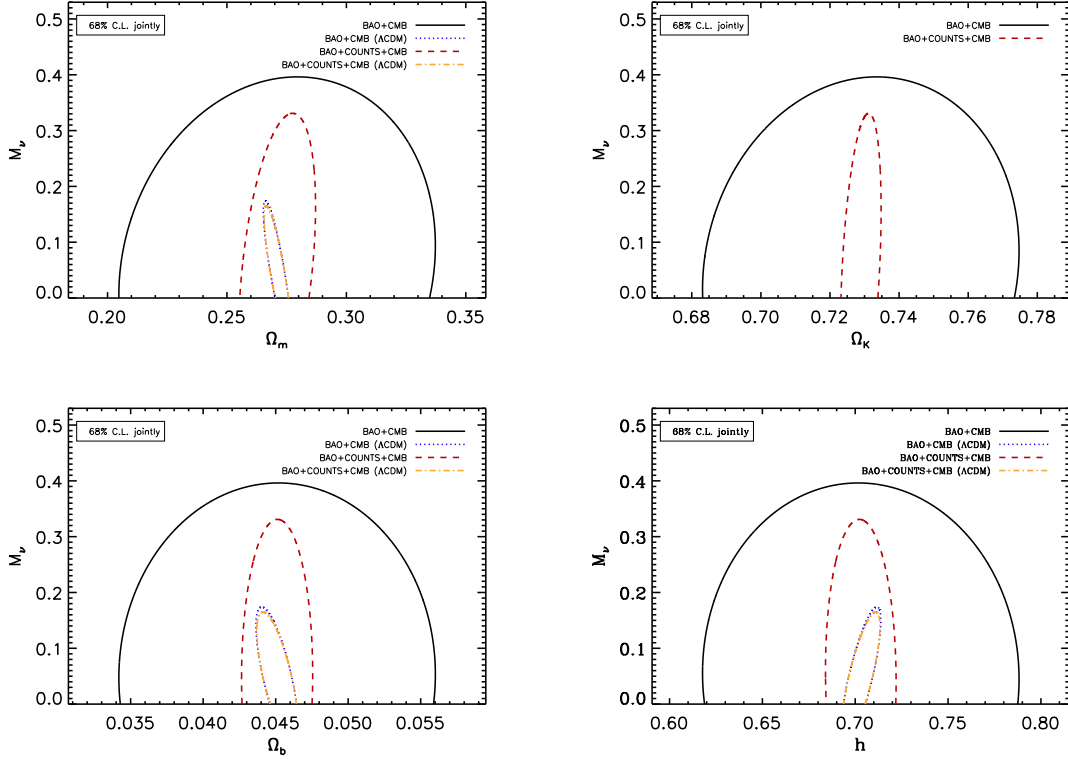


Figure 1: 2-parameter projected 68% C.L. contours in the M_ν - q_α subspace with $q_\alpha = \Omega_m, \Omega_K, \Omega_b, h$. The solid black line and the dotted blue line correspond to BAO+ $P_c(k)$ -shape cluster data from a *Euclid*-like survey in combination with *Planck* priors for a general cosmology, and a Λ CDM Universe, respectively. The dashed red line, and the dot-dashed orange line are obtained with the further addition of cluster counts data, and represent the confidence contours obtained for the two cosmological models, respectively.

of Table 1 show the $1-\sigma$ errors and the values of the r coefficients for the M_ν - q_α correlations obtained in a general cosmology which includes dark energy and curvature, and exploiting information from the combination of BAO+ $P(k)$ -shape extracted from the observed galaxy cluster power spectrum of Eq. (4.1). As stated in Appendix A, we assume that up to $z = 1$ photometrically selected clusters are also spectroscopically confirmed, and consequently we assume a redshift error $\sigma_z = 0.001(1+z)$ for $0.2 < z < 1$, and $\sigma_z = 0.03(1+z)$ for $1 < z < 2$. We have verified that in this case 99.95% of the signal comes from $z < 1$, for both neutrino mass and dark energy parameters w_0 and w_a . This is due to the damping effect on the observed power spectrum caused by the redshift error σ_z which increases linearly with redshift (see Eq. (A.5)). Supposing instead that photometrically selected galaxy clusters could be spectroscopically confirmed up to $z = 2$, this would imply 96% of the signal coming from $z < 1$ as regards neutrino mass constraints, while for errors on the dark energy equation of state, one would get the 99% of the signal in terms figure of merit from $z < 1$. After 2019, future galaxy surveys will probably be able to reach spectroscopic precision on σ_z even for redshifts $z > 1$.

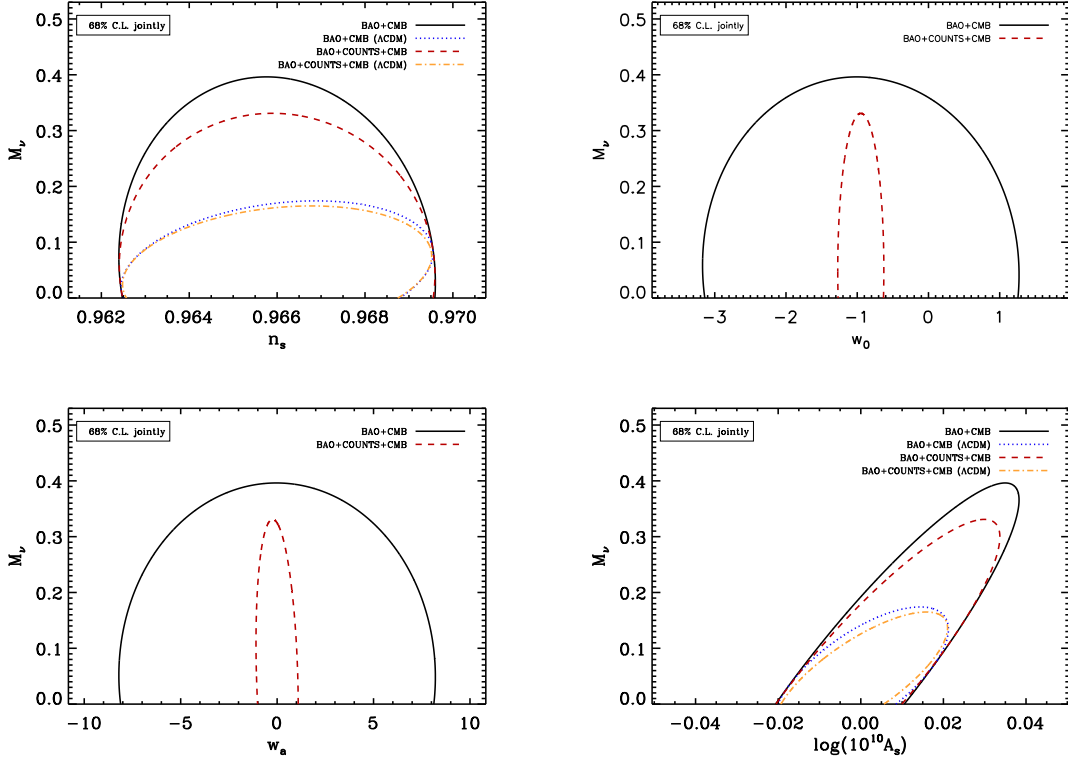


Figure 2: 2-parameter projected 68% C.L. contours in the M_ν - q_α subspace with $q_\alpha = n_s, w_0, w_a, \log(10^{10} A_s)$. The solid black line and the dotted blue line correspond to BAO+ $P_c(k)$ -shape cluster data from a *Euclid*-like survey in combination with *Planck* priors for a general cosmology, and a Λ CDM Universe, respectively. The dashed red line, and the dot-dashed orange line are obtained with the further addition of cluster counts data, and represent the confidence contours obtained for the two cosmological models, respectively.

As we can observe, the marginalised errors of all the cosmological parameters are 1–2 orders of magnitude larger than the corresponding errors obtained from galaxy power spectrum measurements [32]. This is expected and due to the fact that the galaxy cluster spatial density is much lower than the density of spectroscopically selected galaxies from a *Euclid*-like survey, and evidently this effect is not compensated by the larger value of the effective bias. Let us notice that, having marginalised over the cluster power spectrum amplitude and redshift-space distortions, the information from BAO+ $P_c(k)$ -shape does not provide any constraint on $\log(10^{10} A_s)$. In this case the 1 - σ error on the total neutrino mass is quite large, $\sigma(M_\nu) = 2.6$ eV and, except for w_0 , all the cosmological parameters are non-negligibly correlated with M_ν , with the main correlations given by $M_\nu - \Omega_m$, $M_\nu - \Omega_b$, and $M_\nu - h$.

Looking at the 4th and 5th columns of the upper panel of Table 1, we can observe that all the constraints improve considerably, by 1–2 orders of magnitude, when *Planck* priors are added to BAO+ $P_c(k)$ -shape cluster data, except for the dark energy equation of state, owing to the CMB weakness in constraining w_0 and w_a simultaneously. Focusing on the

neutrino mass, in this case $\sigma(M_\nu) = 0.23$ eV and all the parameter degeneracies with M_ν are broken, except for $\log(10^{10} A_s)$, which is now constrained by CMB measurements and is highly degenerate with M_ν , $r = 0.9$, since these two parameters produce opposite effects on the cluster power spectrum.

Let us now consider a less general cosmology, i.e. the Λ CDM model, where the curvature Ω_K and the dark energy equation of state are kept fixed to their fiducial values. Looking at the 2nd column of the lower panel in Table 1, we note that the 1- σ error on the neutrino mass decreases by a factor of ~ 1.5 with respect to the general case, and the combination with *Planck* priors (4th column) gives $\sigma(M_\nu) = 0.08$ eV, which is comparable with the lowest value of the total neutrino mass, $M_\nu = 0.05$ eV, predicted by neutrino oscillation experiments. This means that the combination of CMB data with BAO+ $P_c(k)$ -shape measurements from galaxy clusters, selected from future nearly all-sky galaxy catalogs, could detect values of the neutrino mass close to the minimum one assuming a Λ CDM Universe. Anyway, all the cosmological parameters keep a large correlation with M_ν , implying that information from external data, as e.g. a Gaussian prior on h , could help to further improve the neutrino mass constraint.

5.2 COUNTS+CMB

The cosmological parameter forecasts obtained from cluster counts in a *Euclid*-like galaxy survey are reported in the 6th and 7th columns of the upper panel in Table 1 for a general cosmology, and in the corresponding columns of the lower panel for the Λ CDM case. The four nuisance parameters described in § 2.1 have been marginalised over. The constraining power of cluster counts depends on the considered parameter: for example the 1- σ errors on Ω_m and w_0 are respectively ~ 2.5 and ~ 4 times lower than the ones obtained from cluster BAO+ $P_c(k)$ -shape measurements, for both the model cosmologies. Nonetheless, the constraints on all the remaining cosmological parameters are much worse than the BAO+ $P_c(k)$ -shape forecasts, and in particular the error on the total neutrino mass from cluster counts for the general cosmology, $\sigma(M_\nu) = 28.5$ eV, is ~ 11 times larger than from the cluster power spectrum, while, for the Λ CDM model it is ~ 2.5 times larger, $\sigma(M_\nu) = 4.3$ eV. For cluster counts as well, all the cosmological parameters are highly correlated with M_ν and the larger correlation coefficients r are given by $M_\nu - \Omega_m$, $M_\nu - \Omega_b$, $M_\nu - h$, $M_\nu - n_s$, and $M_\nu - \log(10^{10} A_s)$.

Adding cluster counts data to *Planck* priors breaks degeneracies in CMB measurements, especially for Ω_K , w_0 and w_a , so that cosmological parameter constraints coming from their combination improve considerably when compared to cluster counts alone. Anyway, also in this case, all the cosmological parameters remain strongly correlated with the neutrino mass. For COUNTS+CMB we find $\sigma(M_\nu) = 0.26$ eV for a cosmological model which includes curvature and an evolving dark energy component, and $\sigma(M_\nu) = 0.17$ eV for a Λ CDM cosmology. These findings have to be compared with the corresponding errors from cluster BAO+ $P_c(k)$ -shape measurements, given by $\sigma(M_\nu) = 0.23$ eV and $\sigma(M_\nu) = 0.08$ eV, respectively.

5.3 BAO+COUNTS

Being complementary probes, the separate constraining powers of cluster counts and cluster BAO+ $P_c(k)$ -shape data are notably amplified when combined together. In the case of the present work, the degeneracy breaking, provided by such a combination, is mainly due to the inclusion, in cluster count measurements, of information from the power spectrum amplitude and from the growth of structure (encapsulated in $n(M, z)$), which, on the contrary, are marginalised over for BAO+ $P_c(k)$ -shape measurements. This additional information helps to mitigate the degeneracies between the cosmological parameters, present when each probe is taken individually. Nonetheless, it is worth noting that dN/dz and $P_c(k, z)$ describe different phenomena, abundance and clustering respectively, and have a different dependence on cosmological parameters; for instance, the growth rate of perturbations f_g influences mainly the redshift evolution of cluster abundance, while free-streaming of neutrinos suppresses fluctuation power on small scales, mainly affecting the cluster correlation. Therefore, the inclusion even of amplitude and growth information in cluster power spectrum measurements would improve the cosmological parameter errors, but, anyway, would not replace the role of cluster counts in statistical constraints [76]. Moreover, these two probes are affected by totally different systematics, and this contributes in breaking the degeneracies present in each method.

The qualitative explanation above can be verified by comparing the 10th column of the upper panel of Table 1 with the 2nd and 6th columns. We notice how the $1-\sigma$ errors for Ω_m , Ω_K , Ω_b , h , and $\log(10^{10}A_s)$ are reduced by ~ 1 order of magnitude with respect to the minimum of the corresponding errors from cluster counts and cluster BAO+ $P_c(k)$ -shape measurements taken separately. The decrease is less pronounced but still important for n_s , w_0 , w_a . In particular for the total neutrino mass we find $\sigma(M_\nu) = 0.9$ eV in a general model cosmology, which is comparable to constraints from the Ly α forest at 95% C.L. [24], and $\sigma(M_\nu) = 0.57$ eV in a Λ CDM cosmology (lower panel of Table 1), comparable to constraints from redshift space distortions [43]. The cosmological parameters more strongly correlated with M_ν are in this case Ω_b , h , and $\log(10^{10}A_s)$.

5.4 BAO+COUNTS+CMB

In this Section we consider the total combination of cluster counts and BAO+ $P_c(k)$ -shape measurements with CMB data. The results are shown in the last two columns of Table 1, while Figs. 1-2 represent the 2-parameter projected 68% C.L. contours in the M_ν - q_α subspace. The solid black line and the dotted blue line correspond to BAO+ $P_c(k)$ -shape cluster data from a *Euclid*-like survey in combination with *Planck* priors for a general cosmology, and a Λ CDM Universe, respectively. The dashed red line, and the dot-dashed orange line are obtained from the further addition of cluster counts data, and represent respectively the confidence contours obtained for the two cosmological models. These plots clearly display the contribution of cluster counts in constraining cosmological parameters, and show that the main effect results from breaking degeneracies when the cosmological model includes curvature and an evolving dark energy component (compare the solid black line with the red dashed one), so that the $1-\sigma$ errors decrease by $\sim 4 - 7$ times with re-

spect to the combination CMB+BAO+ $P_c(k)$ -shape for all the parameters, except for n_s , $\log(10^{10}A_s)$, and M_ν . Specifically, for the total neutrino mass error in a general cosmology we find $\sigma(M_\nu) = 0.18$ eV, which reduces to $\sigma(M_\nu) = 0.076$ eV in a Λ CDM Universe⁸. It is worth noting that, in the latter case, all the cosmological parameter constraints are comparable to the corresponding ones as obtained in a general cosmology from the galaxy CMB+BAO+ $P_g(k)$ -shape measurements in a *Euclid*-like spectroscopic galaxy survey [32]. This means that, even if the galaxy clustering constraining power is undoubtedly superior to the galaxy cluster one, the two probes are complementary and their combination could greatly help to improve constraints on all the cosmological parameters, including neutrino mass and dark energy.

Finally, the 2nd and 4th columns of Table 2 show that, fixing the four nuisance parameters A , B , $\sigma_{\ln M,0}$, and β , the 1- σ errors on the total neutrino mass reduce from 0.18 eV to 0.11 eV for a general cosmology, and from 0.076 eV to 0.03 eV for a Λ CDM model. Therefore, if the true underlying cluster masses were known without uncertainties, it would be possible to detect at 3- σ level and measure the mass of cosmic neutrinos in a cosmology-independent way, if the sum of neutrino masses is above 0.3 eV, while assuming spatial flatness and cosmological constant otherwise.

6. Conclusions

In this work we adopted a Fisher matrix approach to forecast constraints on a wide array of cosmological parameters from the photometric galaxy cluster catalog produced by future *Euclid*-like surveys. Specifically, we focused attention on the total mass of neutrinos as derived by a combination of cluster number counts and the shape of the cluster power spectrum, including BAO information. In addition to the cosmological parameters of the standard Λ CDM model and the total neutrino mass, we also considered non-vanishing curvature, as well as a dynamical evolution of the dark energy equation of state. We marginalised our constraints over the growth function, the amplitude of the scalar curvature power spectrum, and a set of nuisance parameters intended to represent the uncertainties in assigning true masses to galaxy clusters. In order to make our analysis more complete, we also added priors on cosmological parameters coming from the ongoing CMB experiment *Planck*. Our main results can be summarised as follows.

- Constraints coming from cluster counts and power spectrum shape+BAO separately are in general relatively weak. Errors on parameter estimated using the cluster correlation function alone are up to two orders of magnitude larger than what is obtained with the galaxy correlation function, due to the lower spatial number density of clusters. Number counts alone do better than this only for the matter density parameter and the present-day dark energy equation of state, while they perform worst in all

⁸For completeness and comparison reasons, we have considered also the case where only photometric redshifts are available. Under this assumption, for the combination CMB+BAO+ $P_c(k)$ -shape we find $\sigma(M_\nu) = 0.24$ eV in a general cosmology, which reduces to $\sigma(M_\nu) = 0.16$ eV in a Λ CDM Universe, i.e. neutrino mass constraints would worsen by a factor ~ 1.3 and ~ 2 , respectively, if a spectroscopic follow-up of galaxy cluster up to $z = 1$ would not be feasible.

other cases. Specifically, the error on the total neutrino mass is $\sigma(M_\nu) = 2.6$ eV for cluster correlation function alone and $\sigma(M_\nu) = 28.5$ eV for cluster counts alone in the context of a general cosmological model including curvature and evolving dark energy.

- Combining the cluster power spectrum shape+BAO with cluster counts exploits the advantages of both approaches, and hence greatly improves the constraints of individual probes. The errors on cosmological parameters estimated by the combination of the two tests are reduced in general very substantially for all parameters, and by up to an order of magnitude for some of them. For a general cosmology, the error on the total neutrino mass is brought down to $\sigma(M_\nu) = 0.9$ eV, comparable with present constraints from the Ly α forest [24] and CMB in non-flat models [16].
- Constraints on cosmological parameters are also greatly tightened by either *i*) adopting *Planck* priors, and *ii*) reducing the number of free parameters by shrinking the cosmological model to a standard Λ CDM one. For a general cosmology, adding *Planck* priors to the cluster power spectrum shape+BAO reduces the parameter errors by 1 – 2 orders of magnitude, except for the dark energy parameters, while performing the same operation on the cluster counts also improves the constraining power by more than one order of magnitude. Moreover, these priors help to remove many of the degeneracies between cosmological parameters, thus reducing the error on the total neutrino mass from either probes down to $\sigma(M_\nu) \sim 0.25$ eV, which goes down to $\sigma(M_\nu) \sim 0.08 - 0.17$ if only a Λ CDM background is considered.
- The combination of cluster counts, power spectrum shape+BAO, and *Planck* priors produces very competitive constraints. In a Λ CDM context, the errors on all cosmological parameters are compatible with those derived for a general cosmology from the galaxy power spectrum shape+BAO performed for the spectroscopic catalog of a future *Euclid*-like survey in combination with *Planck*. Errors on the total neutrino mass are now down to $\sigma(M_\nu) = 0.18$ eV, and $\sigma(M_\nu) = 0.076$ eV if the cosmological model is enforced to be standard Λ CDM. The latter value is only 1.5 times the minimum neutrino mass admitted by neutrino oscillation experiments.
- Fixing the value of the nuisance parameters, which equals assuming a perfect knowledge of cluster true masses, also greatly improves parameter constraints. It is quite unlikely that this level of precision can be reached for all clusters in the *Euclid* photometric catalog, while it might be a reasonable assumption for a subsample of objects having an extensive multi-wavelength follow-up. Nonetheless, if this will indeed be the case, the errors on all estimated parameters would be reduced by up to a factor of a few. Specifically, the error on the total neutrino mass would go down to $\sigma(M_\nu) = 0.1$ eV for the general cosmology and to only $\sigma(M_\nu) = 0.034$ eV for the Λ CDM one, which means that the minimum neutrino mass could be detected.

We emphasize that the analysis presented here is quite conservative from the point of view of the cosmological information, in that it does not include any guidance from the growth

function in the observed galaxy cluster power spectrum, the amplitude of the scalar curvature power spectrum, and the redshift space distortions. At the same time, we assumed throughout this work a Gaussian distribution of initial density and curvature perturbations. It has been repeatedly shown that the primordial non-Gaussianity has a substantial impact on both the number counts of massive galaxy systems and their correlation function [77, 78, 79, 80, 81, 82, 83, 84, 85, 86, 87, 88]. Inclusion of this primordial non-Gaussianity would have the effect of adding at least another parameter to the study, hence loosening somewhat the constraints that have been found here [89].

The present investigation shows in a neat way that, whilst taken at face value the galaxy correlation function is superior to the cluster correlation function, the combination of the two, and of the latter with cluster number counts, can be of invaluable help in breaking the degeneracies between, and hence effectively improving the constraints on, cosmological parameters. Therefore galaxy clusters are expected to play a key role for precision cosmology with future large galaxy surveys, addressing even questions related to fundamental physics such as the value of the neutrino mass.

Acknowledgments

We acknowledge S. Bardelli for useful discussions. We acknowledge financial contributions from contracts ASI-INAF I/023/05/0, ASI-INAF I/088/06/0, ASI I/016/07/0 'COFIS', ASI 'Euclid-DUNE' I/064/08/0, ASI-Uni Bologna-Astronomy Dept. 'Euclid-NIS' I/039/10/0, and PRIN MIUR 'Dark energy and cosmology with large galaxy surveys'.

A. The observed galaxy cluster power spectrum

The Fisher matrix is defined as the second derivative of the natural logarithm of the likelihood surface about the maximum. In the approximation that the posterior distribution for the parameters is a multivariate Gaussian with mean $\boldsymbol{\mu} \equiv \langle \mathbf{x} \rangle$ and covariance matrix $\mathbf{C} \equiv \langle \mathbf{x}\mathbf{x}^t \rangle - \boldsymbol{\mu}\boldsymbol{\mu}^t$, its elements are given by [59, 68, 90, 91]

$$F_{ij} = \frac{1}{2} \text{Tr} \left[\mathbf{C}^{-1} \frac{\partial \mathbf{C}}{\partial \theta_i} \mathbf{C}^{-1} \frac{\partial \mathbf{C}}{\partial \theta_j} \right] + \frac{\partial \boldsymbol{\mu}^t}{\partial \theta_i} \mathbf{C}^{-1} \frac{\partial \boldsymbol{\mu}}{\partial \theta_j}. \quad (\text{A.1})$$

where \mathbf{x} is a N -dimensional vector representing the data set, whose components x_i are the fluctuations in the galaxy cluster density relative to the mean in N disjoint cells that cover the three-dimensional survey volume in a fine grid. The $\{\theta_i\}$ denote the cosmological parameters within the assumed fiducial cosmology. In the limit where the survey volume is much larger than the scale of any features in the observed galaxy cluster power spectrum, it has been shown [69] that it is possible to redefine x_n in Eq. (A.1) to be not the density fluctuation in the n^{th} spatial volume element, but the average power measured with the FKP method [92] in a thin shell of radius k_n in Fourier space.

In order to explore the cosmological parameter constraints from a given galaxy cluster survey, we need to specify the measurement uncertainties of the cluster power spectrum.

Therefore, the statistical error on the measurement of the galaxy cluster power spectrum $P_c(k)$ at a given wave-number bin is [92]

$$\left[\frac{\Delta P_c}{P_c}\right]^2 = \frac{2(2\pi)^2}{V_{\text{survey}}k^2\Delta k\Delta\mu} \left[1 + \frac{1}{n_c P_c}\right]^2, \quad (\text{A.2})$$

where n_c is the mean number density of galaxy clusters given by Eq. (2.7), V_{survey} is the comoving survey volume of the galaxy cluster survey, and μ is the cosine of the angle between \mathbf{k} and the line-of-sight direction $\mu = \vec{k} \cdot \hat{r}/k$.

Actually, the *observed* galaxy cluster power spectrum can be different from the *true* spectrum, and it can be reconstructed assuming a reference cosmology (which we consider to be our fiducial cosmology) as (e.g. [60])

$$P_{\text{obs}}(k_{\text{ref}\perp}, k_{\text{ref}\parallel}, z) = \frac{D_A(z)_{\text{ref}}^2 H(z)}{D_A(z)^2 H(z)_{\text{ref}}} P_c(k_{\text{ref}\perp}, k_{\text{ref}\parallel}, z) + P_{\text{shot}}, \quad (\text{A.3})$$

where

$$P_c(k_{\text{ref}\perp}, k_{\text{ref}\parallel}, z) = b_e^2(z) \left[1 + \beta(z, k) \frac{k_{\text{ref}\parallel}^2}{k_{\text{ref}\perp}^2 + k_{\text{ref}\parallel}^2}\right]^2 \times P_L(k, z). \quad (\text{A.4})$$

In Eq. (A.3), $H(z)$ and $D_A(z)$ are the Hubble parameter and the angular diameter distance, respectively, and the prefactor $(D_A(z)_{\text{ref}}^2 H(z))/(D_A(z)^2 H(z)_{\text{ref}})$ encapsulates the geometrical distortions due to the Alcock-Paczynski effect [60, 93, 94]. Their values in the reference cosmology are distinguished by the subscript ‘ref’, while those in the true cosmology have no subscript. k_{\perp} and k_{\parallel} are the wave-numbers across and along the line of sight in the true cosmology, and they are related to the wave-numbers calculated assuming the reference cosmology by $k_{\text{ref}\perp} = k_{\perp} D_A(z)/D_A(z)_{\text{ref}}$ and $k_{\text{ref}\parallel} = k_{\parallel} H(z)_{\text{ref}}/H(z)$. P_{shot} is the unknown white shot noise that remains even after the conventional shot noise of inverse number density has been subtracted [60], and which could arise from clustering bias even on large scales due to local bias [96]. In Eq. (A.4), $b_e(z)$ is the *effective bias* of Eq. (2.3) between galaxy clusters and matter density distributions, and $\beta(z, k) = f_g(z, k)/b_e(z)$ is the linear redshift-space distortion parameter [97], which in the presence of massive neutrinos depends on both redshift and wave-numbers, since in this case the linear growth rate $f_g(z, k)$ is *scale dependent* even at the linear level. We estimate $f_g(z, k)$ using the fitting formula of Ref. [57]. For the linear matter power spectrum $P_L(k, z)$, we can encapsulate the effect of massive neutrino free-streaming into a *redshift dependent* total matter linear transfer function $T(k, z)$ [98, 99, 100], so that $P_L(k, z)$ in Eq. (A.3) takes the form

$$P_L(k, z) = \frac{8\pi^2 c^4 k_0 A_s}{25 H_0^4 \Omega_m^2} T^2(k, z) \left[\frac{G(z)}{G(z=0)}\right]^2 \left(\frac{k}{k_0}\right)^{n_s} e^{-k^2 \mu^2 \sigma_r^2}, \quad (\text{A.5})$$

where $G(z)$ is the usual *scale independent* linear growth factor in the absence of massive neutrino free-streaming, i.e. for $k \rightarrow 0$ (see Eq. (25) in Ref. [100]), whose fiducial value in each redshift bin is computed through numerical integration of the differential equations governing the growth of linear perturbations in the presence of dark energy [101]. The

redshift-dependent linear transfer function $T(k, z)$ depends on matter, baryon and massive neutrino densities (neglecting dark energy at early times), and is computed in each redshift bin using CAMB⁹ [46].

In Eq. (A.5) we have added the damping factor $e^{-k^2\mu^2\sigma_r^2}$, due to redshift uncertainties, where $\sigma_r = (\partial r/\partial z)\sigma_z$, $r(z)$ being the comoving distance [60, 102]. Here we adopt $\sigma_z = 0.001(1+z)$, for $0.2 < z < 1$, and $\sigma_z = 0.03(1+z)$ for $1 < z < 2$ [33], since we assume that photometrically selected clusters will be confirmed also spectroscopically for low redshifts.

The power spectrum of primordial curvature perturbations, $P_{\mathcal{R}}(k)$, is

$$\Delta_{\mathcal{R}}^2(k) \equiv \frac{k^3 P_{\mathcal{R}}(k)}{2\pi^2} = A_s \left(\frac{k}{k_0}\right)^{n_s}, \quad (\text{A.6})$$

where $k_0 = 0.002/\text{Mpc}$, $A_s = 2.525 \times 10^{-9}$ is the dimensionless amplitude of the primordial curvature perturbations evaluated at a pivot scale k_0 , and n_s is the scalar spectral index [52].

Finally, to minimize nonlinear effects, in our Fisher matrix analysis we restrict wavenumbers to the quasi-linear regime, so that, for $z < 1$, k_{max} is given by requiring that the variance of matter fluctuations in a sphere of radius R is $\sigma^2(R) = 0.25$ for $R = \pi/(2k_{\text{max}})$. This gives $k_{\text{max}} \simeq 0.1h \text{ Mpc}^{-1}$ at $z = 0$ and $k_{\text{max}} \simeq 0.2h \text{ Mpc}^{-1}$ at $z = 1$, well within the quasi-linear regime. In addition, for $1 < z < 2$, we choose $k_{\text{max}} = 0.03h \text{ Mpc}^{-1}$. Finally, in all the calculations we impose $k_{\text{min}} = 10^{-4}h/\text{Mpc}$.

B. The *Planck* Fisher matrix

In this work we use the *Planck* mission parameter constraints as CMB priors, by estimating the cosmological parameter errors via measurements of the temperature and polarization power spectra. As CMB anisotropies, with the exception of the integrated Sachs-Wolfe effect, are not able to constrain the equation of state of dark energy (w_0, w_a)¹⁰, we follow the prescription laid out by DETF [103, 104].

We do not include any B-mode in our forecasts and assume no tensor mode contribution to the power spectra. We use the 100 GHz, 143 GHz, and 217 GHz channels as science channels. These channels have a beam of $\theta_{\text{fwhm}} = 9.5'$, $\theta_{\text{fwhm}} = 7.1'$, and $\theta_{\text{fwhm}} = 5'$, respectively, and sensitivities of $\sigma_T = 2.5\mu\text{K}/K$, $\sigma_T = 2.2\mu\text{K}/K$, $\sigma_T = 4.8\mu\text{K}/K$ for temperature, and $\sigma_P = 4\mu\text{K}/K$, $\sigma_P = 4.2\mu\text{K}/K$, $\sigma_P = 9.8\mu\text{K}/K$ for polarization, respectively. We take $f_{\text{sky}} = 0.80$ as the sky fraction in order to account for galactic obstruction, and use a minimum ℓ -mode $\ell_{\text{min}} = 30$ in order to avoid problems with polarization foregrounds and not to include information from the late Integrated Sachs-Wolfe effect, which depends on the specific dark energy model. We discard temperature and polarization data at $\ell > 2000$ to reduce sensitivity to contributions from patchy reionisation and point source contamination (see [103] and references therein).

⁹<http://camb.info/>

¹⁰On the contrary, using (w_0, w_a) as model parameters to compute the CMB Fisher matrix could artificially break existing degeneracies.

We assume a fiducial cosmology with an anti-correlated isocurvature contribution, varying dark energy and curvature. Therefore we choose the following set of parameters to describe the temperature and polarization power spectra $\boldsymbol{\theta} = (\omega_m, \omega_b, M_\nu, 100 \times \theta_S, \log(10^{10} A_s), n_S, w_0, w_a)$, where θ_S is the angular size of the sound horizon at last scattering and w_0 and w_a are the dark energy parameters according to the CPL parametrization of the dark energy equation of state $w(z) = w_0 + w_a z/(1+z)$.

The Fisher matrix for CMB power spectrum is given by [105, 106]:

$$F_{ij}^{\text{CMB}} = \sum_l \sum_{X,Y} \frac{\partial C_{X,l}}{\partial \theta_i} \text{COV}_{XY}^{-1} \frac{\partial C_{Y,l}}{\partial \theta_j}, \quad (\text{B.1})$$

where θ_i are the parameters to constrain, $C_{X,l}$ is the harmonic power spectrum for the temperature-temperature ($X \equiv TT$), temperature-E-polarization ($X \equiv TE$) and the E-polarization-E-polarization ($X \equiv EE$) power spectrum. The covariance COV_{XY}^{-1} of the errors for the various power spectra is given by the fourth moment of the distribution, which under Gaussian assumptions is entirely given in terms of the $C_{X,l}$ with

$$\text{COV}_{T,T} = f_\ell (C_{T,l} + W_T^{-1} B_l^{-2})^2 \quad (\text{B.2})$$

$$\text{COV}_{E,E} = f_\ell (C_{E,l} + W_P^{-1} B_l^{-2})^2 \quad (\text{B.3})$$

$$\text{COV}_{TE,TE} = f_\ell \left[C_{TE,l}^2 + (C_{T,l} + W_T^{-1} B_l^{-2}) (C_{E,l} + W_P^{-1} B_l^{-2}) \right] \quad (\text{B.4})$$

$$\text{COV}_{T,E} = f_\ell C_{TE,l}^2 \quad (\text{B.5})$$

$$\text{COV}_{T,TE} = f_\ell C_{TE,l} (C_{T,l} + W_T^{-1} B_l^{-2}) \quad (\text{B.6})$$

$$\text{COV}_{E,TE} = f_\ell C_{TE,l} (C_{E,l} + W_P^{-1} B_l^{-2}), \quad (\text{B.7})$$

where $f_\ell = 2/((2\ell + 1)f_{\text{sky}})$, $W_{T,P} = \sum_c W_{T,P}^c$, $W_{T,P}^c = (\sigma_{T,P}^c \theta_{\text{fwhm}}^c)^{-2}$ being the weight per solid angle for temperature and polarization respectively, with a $1-\sigma$ sensitivity per pixel of $\sigma_{T,P}^c$ and a beam of θ_{fwhm}^c extent, for each frequency channel c . The beam window function is given in terms of the full width half maximum (fwhm) beam width by $B_\ell^2 = \sum_c (B_\ell^c)^2 W_{T,P}^c / W_{T,P}$, where $(B_\ell^c)^2 = \exp(-\ell(\ell+1)/(l_s^c)^2)$, $l_s^c = (\theta_{\text{fwhm}}^c)^{-1} \sqrt{8 \ln 2}$ and f_{sky} is the sky fraction [107].

We then calculate the *Planck* CMB Fisher matrix with the help of the publicly available CAMB code [46]. Finally, we transform the *Planck* Fisher matrix for the DETF parameter set to the final parameter sets \mathbf{q} considered in this work (see § 4), using the transformation

$$F_{\alpha\beta}^{\text{CMB}} = \sum_{ij} \frac{\partial \theta_i}{\partial q_\alpha} F_{ij}^{\text{CMB}} \frac{\partial \theta_j}{\partial q_\beta}. \quad (\text{B.8})$$

References

- [1] Lesgourgues, J., Pastor, S. 2006, *Phys. Rep.*, 429, 307
- [2] Wong, Y. Y. Y. 2011, *Ann. Rev. Nucl. Part. Sc.*, 61, 69-98, [arXiv:1111.1436](#)
- [3] Abazajian, K. N., et al. 2011, *Astrop. Phys.*, 35, 177, [arXiv:1103.5083](#)
- [4] Joudaki, S., Kaplinghat, M. 2011, [arXiv:1106.0299](#)

- [5] Joudaki, S. 2012, [arXiv:1202.0005](#)
- [6] Riemer-Sørensen, S. et al. 2011, [arXiv:1112.4940](#)
- [7] Takada, M., Komatsu, E., Futamase, T. 2006, *Phys. Rev. D*, 73, 083520
- [8] Doroshkevich, A. G., Khlopov, M. I., Sunyaev, R. A., Szalay, A. S., Zeldovich, I. B. 1981, *Ann. N. Y. Acad. Sci.*, 375, 32
- [9] Hu, W., Eisenstein, D. J., Tegmark, M. 1998, *Phys. Rev. Lett.*, 80, 5255
- [10] Abazajian, K., Switzer, E. R., Dodelson, S., Heitmann, K., Habib, S. 2005, *Phys. Rev. D* , 71, 043507
- [11] Kiakotou, A., Elgarøy, O., Lahav, O. 2008, *Phys. Rev. D*, 77, 063005
- [12] Brandbyge, J., Hannestad, S., Haugbølle, T., Wong, Y. Y. Y. 2010, *J. Cosm. AstroPart. Phys.*, 9, 14
- [13] Bird, S., Viel, M., Haehnelt, M. J. 2011, [arXiv:1109.4416](#)
- [14] Ichiki, K., Takada, M. 2011, [arXiv:1108.4688](#)
- [15] Komatsu, E., et al. 2010, [arXiv:1001.4538](#)
- [16] Smith, A., Archidiacono, M., Cooray, A., De Bernardis, F., Melchiorri, A., Smidt, J. 2011, [arXiv:1112.3006](#)
- [17] Perotto, L., Lesgourgues, J., Hannestad, S., Tu, H., Wong, Y. Y. Y. 2006, , 10, 13
- [18] Kitching, T. D., Heavens, A. F., Verde, L., Serra, P., Melchiorri, A., 2008, *Phys. Rev. D*, 77, 103008
- [19] Wang, S., Haiman, Z., Hu, W., Khoury, J., May, M. 2005, *Phys. Rev. Lett.*, 95, 011302
- [20] Vikhlinin, A., Kravtsov, A. V., Burenin, R. A., Ebeling, H., Forman, W. R., Hornstrup, A., Jones, C., Murray, S. S., Nagai, D., Quintana, H., Voevodkin, A. 2009, *Astrophys. J.*, 692, 1060
- [21] Thomas, S. A., Abdalla, F. B., Lahav, O. 2010, *Phys. Rev. Lett.*, 105, 031301
- [22] Gonzalez-Garcia, M. C., Maltoni, M., Salvado, J. 2010, *J. High Energy Phys.*, 8, 117
- [23] Reid, B. A., et al. 2010, *Mont. Not. Roy. Astron. Soc.*, 404, 60
- [24] Viel, M., Haehnelt, M. G., Springel, V. 2010, *J. Cosm. AstroPart. Phys.*, 06, 015, [arXiv:1003.2422](#)
- [25] Seljak, U., Slosar, A., McDonald, P. 2006, *J. Cosm. AstroPart. Phys.*, 10, 14
- [26] Goobar, A., Hannestad, S., Mörtzell, E., Tu H. 2006, *J. Cosm. AstroPart. Phys.*, 6, 19
- [27] Gratton, S., Lewis, A., Efstathiou, G. 2008, *Phys. Rev. D*, 77, 083507
- [28] Hannestad, S., Wong, Y. Y. Y. 2007, *J. Cosm. AstroPart. Phys.*, 7, 4
- [29] Abell, P. A., Allison, J., Anderson, S. F., Andrew, J. R., Angel, J. R. P., Armus, L., Arnett, D., Asztalos, S. J., Axelrod T. S., et al. 2009, [arXiv:0912.0201](#)
- [30] Hannestad, S. 2010, *Prog. Part. Nuc. Phys.*, 65, 185
- [31] Lahav, O., Kiakotou, A., Abdalla, F. B., Blake, C. 2010, *Mont. Not. Roy. Astron. Soc.*, 405, 168

- [32] Carbone, C., Verde, L., Wang, Y., Cimatti A. 2011 *J. Cosm. AstroPart. Phys.*, 03, 030, [arXiv:1012.2868](#)
- [33] Laureijs R., et al. 2011, [arXiv:1110.3193](#)
- [34] Bahcall, N. A. and Soneira, R. M. 1983, *Astrophys. J.*, 270, 20
- [35] Bahcall, N. A., Batuski, D. J. and Olowin, R. P. 1988, *Astrophys. J.*, 333, L13
- [36] Carlberg, R. G. et al. 1996, *Astrophys. J.*, 462, 32
- [37] Donahue, M. et al. 1998 *Astrophys. J.*, 502, 550
- [38] Giusarma, E., Corsi, M., Archidiacono, M., de Putter R., Melchiorri, A., Mena, O., Pandolfi, S. 2011, *Phys. Rev. D*, 83, 115023
- [39] Gonzalez-Morales, A. X., Poltis, R., Sherwin, B. D., Verde, L. 2011, [arXiv:1106.5052](#)
- [40] Sheth, R. K. & Tormen, G. 2002, *Mont. Not. Roy. Astron. Soc.*, 329, 61
- [41] Percival, W. J. 2005, *Astron. Astrophys.*, 443, 819, [arXiv:astro-ph/0508156](#)
- [42] Wang, L., & Steinhardt, P. J. 1998, *Astrophys. J.*, 508, 483
- [43] Marulli, F., Carbone, C., Viel, M., Moscardini, L., Cimatti, A. 2011, *Mont. Not. Roy. Astron. Soc.*, 418, 346, [arXiv:1103.0278](#)
- [44] Jose, C. , Samui, S., Subramanian, K., Srianand, R. 2011, *Phys. Rev. D* , 83, 123518
- [45] Sheth, R. K., Mo, H. ., Tormen, G. 2001, *Mont. Not. Roy. Astron. Soc.*, 323, 1
- [46] Lewis, A., Challinor, A., Lasenby, A. 2000, *Astrophys. J.*, 538, 473
- [47] Lima, M. & Hu, W. 2005 *Phys. Rev. D*, 72, 043006
- [48] Abramowitz, M. & Stegun, I. A. “Handbook of Mathematical Functions”, Editor: Abramowitz, M. & Stegun, New York: Dover, 1972
- [49] Johnston, D. E., et al. 2007, [arXiv:0709.1159](#)
- [50] Rykoff, E. S., et al. 2011, [arXiv:1104.2089](#)
- [51] Tinker, J. L., et al. 2011, [arXiv:1104.1635](#)
- [52] D. Larson 2011, *Astrophys. J. Suppl.*, 192, 16
- [53] Mangano, G., Miele, G., Pastor, S., Pinto, T., Pisanti, O., Serpico P. D. 2005, *Nucl.Phys. B*, 729, 221
- [54] Chevallier, M., & Polarski, D. 2001, *Int. J. Mod. Phys. D*, 10, 213
- [55] Linder, E. ., 2003, *Phys. Rev. Lett.*, 90, 091301
- [56] Saito, S., Takada, M., Taruya, A. 2009, *Phys. Rev. D*, 80, 083528
- [57] Kiakotou, A., Elgaroy, O., & Lahav, O. 2008, *Phys. Rev. D*, 77, 063005
- [58] Wang, Y., & Tegmark, M. 2004, *Phys. Rev. Lett.*, 92, 241302, [arXiv:astro-ph/0403292](#)
- [59] R. A. Fisher 1935, *J. Roy. Stat. Soc.*, 98, 39
- [60] Seo, H. J., & Eisenstein, D. J. 2003, *Astrophys. J.*, 598, 720
- [61] Wang, Y. 2006, *Astrophys. J.*, 647, 1, [arXiv:astro-ph/0601163](#)

- [62] Wang, Y. 2008, *J. Cosm. AstroPart. Phys.*, 05, 021, [arXiv:0710.3885](#)
- [63] Wang, Y., et al 2010, *Mont. Not. Roy. Astron. Soc.*, 409, 737, [arXiv:1006.3517](#)
- [64] Carbone, C., Mangilli, A., Verde, L. 2011, *J. Cosm. AstroPart. Phys.*, 09, 028, [arXiv:1107.1211](#)
- [65] Amendola, L., Pettorino, V., Quercellini, C., Vollmer, A. 2011, [arXiv:1111.1404](#)
- [66] Di Porto, C., Amendola, L., Branchini, E. 2012, *Mont. Not. Roy. Astron. Soc.*, 419, 985
- [67] Di Porto, C., Amendola, L., Branchini, E. 2012, [arXiv:1201.2455](#)
- [68] Tegmark, M., Taylor A., Heavens A. 1997, *Astrophys. J.*, 480, 22
- [69] Tegmark, S. 1997, *Phys. Rev. Lett.*, 79, 3806
- [70] Wang, Y. 2008, *Phys. Rev. D*, 77, 123525
- [71] Holder, G., Haiman, Z., Mohr, J. J. 2001 *Astrophys. J. Lett.*, 560, L111
- [72] Majumdar, S. & Mohr, J. J. 2003, *Astrophys. J.*, 585, 603
- [73] Sartoris, B., Borgani, S., Fedeli, C., Matarrese, S., Moscardini, L., Rosati, P., Weller, J. 2010, *Mont. Not. Roy. Astron. Soc.*, 407, 2339
- [74] Sartoris, B., Borgani, S., Rosati, P., Weller, J. 2011, [arXiv:1112.0327](#)
- [75] Shimon, M., Sadeh, S., Rephaeli, Y. 2011, *Mont. Not. Roy. Astron. Soc.*, 412, 1895, [arXiv:1009.4110](#)
- [76] Wang, S., Khoury, J., Haiman, Z., May, M. 2004, *Phys. Rev. D*, 70, 123008
- [77] Slosar, A., Hirata, C., Seljak, U., Ho, S., Padmanabhan, N. 2008, *J. Cosm. AstroPart. Phys.*, 08, 031
- [78] Grossi, M., Verde, L., Carbone, C., Dolag, K., Branchini, E., Iannuzzi, F., Matarrese, S., Moscardini, L. 2009, *Mon. Not. Roy. Astron. Soc.*, 398, 321
- [79] Grossi, M., Dolag, K., Branchini, E., Matarrese, S., Moscardini, L. 2007, *Mon. Not. Roy. Astron. Soc.*, 382, 1261
- [80] Grossi, M., Branchini, E., Dolag, K., Matarrese, S., Moscardini, L. 2008, *Mon. Not. Roy. Astron. Soc.*, 390, 438
- [81] Pillepich, A., Porciani, C., Hahn, O. 2010, *Mon. Not. Roy. Astron. Soc.*, 402, 191
- [82] Desjacques, V., Seljak, U., Iliev, I. T. 2009, *Mont. Not. Roy. Astron. Soc.*, 396, 85
- [83] Dalal, N., Dor, O., Huterer, D., Shirokov, A. 2008, *Phys. Rev. D* 77, 123514
- [84] Maggiore, M., Riotto, A. 2010, *Astrophys. J.*, 717, 526
- [85] Matarrese, S., Verde, L. 2008, *Astrophys. J. Lett.*, 677, L77
- [86] Lam, T. Y., Sheth, R. K., Desjacques, V. 2009, *Mont. Not. Roy. Astron. Soc.*, 399, 1482
- [87] D'Amico, G., Musso, M., Norea, J., Paranjape, A. 2011, *J. Cosm. AstroPart. Phys.*, 02, 001
- [88] McDonald, P. 2008, *Phys. Rev. D*, 78,123519
- [89] Carbone, C., Mena, O., Verde, L. 2010, *J. Cosm. AstroPart. Phys.*, 07, 020
- [90] Vogeley, M. S. & Szalay, A. S. 1996 *Astrophys. J.*, 465, 43

- [91] Jungman, G., Kamionkowski, M., Kosowsky, A., Spergel, D. 1996, *Phys. Rev. D*, 54, 1332
- [92] Feldman, H. A., Kaiser, N., Peacock, J. A. 1994, *Astrophys. J.*, 426, 23
- [93] Ballinger, W. E., Peacock, J. A., Heavens, A. F. 1996, *Mont. Not. Roy. Astron. Soc.*, 282, 877
- [94] Marulli, F., Bianchi, D., Branchini, E., Guzzo, L., Moscardini, L. in prep.
- [95] Eisenstein, D. J., & Hu, W. 1998, *Astrophys. J.*, 496, 605
- [96] Seljak, U. 2000, *Mont. Not. Roy. Astron. Soc.*, 318, 203
- [97] Kaiser, N. 1987, *Mont. Not. Roy. Astron. Soc.*, 227, 1
- [98] Takada, M., Komatsu, E., Futamase, T. 2006, *Phys. Rev. D*, 73, 083520
- [99] Takada, M. 2006, *Phys. Rev. D*, 74, 043505
- [100] Eisenstein, D., J., & Hu, W. 1997, *Astrophys. J.*, 511, 5
- [101] Linder, E. V. & Jenkins, A. 2003, *Mont. Not. Roy. Astron. Soc.*, 346, 573
- [102] Wang, Y. 2010, *Mod. Phys. Lett. A*, 25, 3093
- [103] Albrecht, A., et al. 2006, [arXiv:astro-ph/0609591](https://arxiv.org/abs/astro-ph/0609591)
- [104] Rassat, A., Amara, A., Amendola, L., Castander, F. J., Kitching, T., Kunz, M., Refregier, A., Wang, Y., Weller, J. 2008, [arXiv:0810.0003](https://arxiv.org/abs/0810.0003)
- [105] Zaldarriaga M., Seljak U. 1997, *Phys. Rev. D*, 55, 1830
- [106] Zaldarriaga M., Spergel D. N., Seljak U. 1997, *Astrophys. J.*, 488, 1
- [107] Bond, J. R., Efstathiou, G., Tegmark, M. 1997, *Mont. Not. Roy. Astron. Soc.*, 291, L33